



Communication

Non-destructive tomographic energy-dispersive diffraction imaging of the interior of bulk concrete

Christopher Hall^a, Sally L. Colston^b, Andrew C. Jupe^b, Simon D.M. Jacques^b,
Richard Livingston^c, Alsaïd O.A. Ramadan^d, Amde W. Amde^d, Paul Barnes^{b,*}

^aCentre for Materials Science and Engineering, School of Mechanical Engineering, King's Building, Edinburgh ED9 3JL, UK

^bIndustrial Materials Group, Department of Crystallography, Birkbeck College, Malet Street, London WC1E 7HX, UK

^cOffice of Infrastructure R&D, Federal Highway Administration, McLean, VA, USA

^dDepartment of Civil Engineering, University of Maryland, College Park, MD, USA

Received 9 September 1999; accepted 3 January 2000

Abstract

A new tomographic technique, termed TEDDI (tomographic energy-dispersive diffraction imaging) has recently been invented by Hall et al. [C. Hall, P. Barnes, J.K. Cockcroft, S.L. Colston, D. Hausermann, S.D.M. Jacques, A.C. Jupe, M. Kunz, Synchrotron radiation energy-dispersive diffraction tomography, Nucl Instrum Methods Res, Sect B 140 (1998) 253–257; C. Hall, P. Barnes, J.K. Cockcroft, S.D.M. Jacques, A.C. Jupe, X. Turrillas, M. Hanfland, D. Hausermann, Rapid whole-rock mineral analysis and composition mapping by synchrotron X-ray diffraction, Anal Commun 33 (1996) 245–248] and applied to cementitious systems. TEDDI has notable unique features in that: it exploits *diffraction*, rather than *spectroscopic* sensing, and therefore directly yields compositional/structural information about the sample; the diffracting region can be made small or large depending on application, the ultimate spatial resolution being in the micron range; with the use of energetic (20–125 keV) synchrotron beams, bulk objects such as concrete blocks can be penetrated so that the technique becomes *non-destructive*. We report on early tests of this technique as a means to non-destructively examine the interior of concrete prism specimens. Concrete, by definition, is a heterogeneous material because it contains coarse aggregates on a length scale of ~ 1 cm. This is orders of magnitude larger than the effective penetration depth of conventional X-ray diffraction systems (typically <100 μm at 1.54 Å) which, therefore, cannot probe the interior of intact concrete specimens. It is possible to pulverize concrete, sift out the aggregates, and analyze the remaining fraction but the degree of representation of such powders is questioned since certain phases may be lost or enriched during this process; furthermore, the spatial distribution of the analyzed phases within the concrete will be lost and, with it, important information such as whether the phase in question forms in the cement paste matrix or at the aggregate interface. Even after these limitations, conventional diffraction/microscopy analysis is at best a “one shot” process in time. The TEDDI technique has the promise to avoid all these problems by enabling the examination of intact concrete specimens on the length scale of several centimeters. © 2000 Elsevier Science Inc. All rights reserved.

Keywords: Characterization; Image analysis; X-ray diffraction; Concrete; Synchrotron

1. Tomographic energy-dispersive diffraction imaging (TEDDI)

TEDDI has been developed from *energy-dispersive diffraction*, a technique which has already found wide application in the field of time-resolved in-situ diffraction studies of materials such as catalysts and zeolites [2,3], ceramics [4],

cements [5,6], and rocks [1,7]. The basis of the technique is illustrated in the schematic Fig. 1. A hard (e.g., 20–125 keV) highly collimated X-ray beam obtained from a synchrotron source is directed onto a specimen of interest. Because such a beam is *white* (i.e., a wavelength/energy continuum) a diffraction pattern can, according to Bragg's law ($\lambda = 2d \sin\theta$), be collected at any single scattering angle, 2θ , provided the wavelengths, λ , of the diffracted X-ray photons can be determined. This is done in practice using energy-dispersive detectors, since X-ray wavelength is inversely related to the photon energy ($\lambda = 12.4/E$, λ being in

* Corresponding author. Tel.: +44-20-7631-6817; fax: +44-20-7631-6803.

E-mail address: barnes@img.cryst.bbk.ac.uk (P. Barnes).

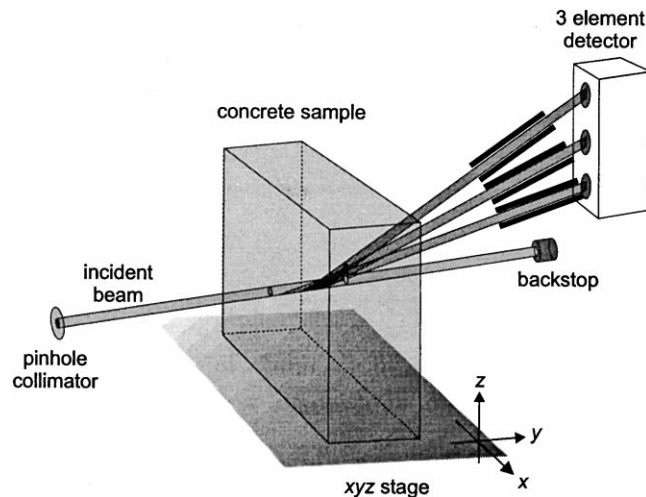


Fig. 1. Schematic illustrating the basic mode of action of the TEDDI configuration in relation to the three energy-dispersive detectors and the concrete sample under study. The incident beam defines, with each diffracted beam, three diffraction lozenges which are then aligned into coincidence. The TEDDI maps in this study were obtained by first aligning the concrete sample with the y -traverse so that the lozenges fell just inside the concrete sample and then traversing the concrete sample along x and z to obtain a 2D TEDDI map.

units of angströms (\AA) and E in kilo-electron-volts (keV)), and the diffraction pattern then becomes a plot of intensity versus photon energy, E , rather than versus angle, 2θ . Since the energy-dispersive method is a *fixed geometry* technique, with the incident and diffracted X-ray beams defined by the slit/collimator system, the diffracted signal is seen to originate from a precise region termed a *lozenge* (see Fig. 1). This region can be made large ($\sim 1 \text{ mm}^3$) or small ($\sim 10,000 \text{ }\mu\text{m}^3$) by appropriate manipulation [8] of the X-ray beam slits, collimation system, and diffracting angle, 2θ ; this is a distinguishing feature of TEDDI from neutron diffraction techniques which, while possessing similar attributes of penetration, cannot compete in terms of spatial resolution. The particular novelty with TEDDI is to arrange so that the diffraction-lozenge is scanned through the specimen, collecting EDD patterns at each point. The scanning procedure is performed by mechanically moving the specimen through the stationary synchrotron white X-ray beam, the scanning being either one-, two- or three-dimensional (1D, 2D, 3D, respectively) in nature. In this study, *three* energy-dispersive detectors were used (see Fig. 1) with the result that three separate diffraction patterns were collected simultaneously from substantially the same sample region. Since these three detectors cover different ranges of reciprocal space, the overall diffraction information becomes extended, this being a particularly desirable feature in the case of multi-phase materials such as cement/concrete.

2. A prototype tomographic study of concrete

A prototype study has been undertaken of the potential of TEDDI to non-destructively examine bulk concrete objects.

In this first study, the emphasis was on assessing the technique's capability to non-destructively examine cementitious material on a relatively coarse scale. The concrete sample used in this study was produced as part of a research project to develop an improved method of measuring the damage associated with delayed ettringite formation [9]. Three batches of concrete, made with the same Type III Portland cement, were mixed with varying levels of potassium (0.7%, 1.4%, and 2.1% K_2O). The fine aggregate was Maryland quartz sand and the coarse aggregate Frederick Maryland limestone. The concrete batches were then cast into both $3 \times 3 \times 11.25$ -in. prisms and 4×8 -in. cylinders. Some of the specimens were cured at elevated temperatures and the others at room temperature. From some of the prisms, 1-in. diameter cores were drilled according to the Duggan test procedure [10]. The cylinders, cores, and complete prisms were exposed to the standard Duggan test temperature cycles to induce microcracking, and then immersed in a room temperature water bath. Periodically, the linear expansion of the specimens was measured with a length comparator according to ASTM C490. The steam-cured specimens with the highest potassium content achieved 1% expansion at 65 days compared to 115 days for the lowest potassium content. The compressive strengths at the end of the test period were around 5 and 20 MPa, respectively [11].

Examination of fracture surfaces with the scanning electron microscope and EDAX revealed abundant amounts of ettringite in cracks and at aggregate interfaces at all levels of potassium content. The presence of thaumasite was also suspected. It was not possible from the SEM examination to establish if the amount of ettringite correlated with the potassium content. To make this correlation, it would be necessary to quantify the amount of ettringite over the entire

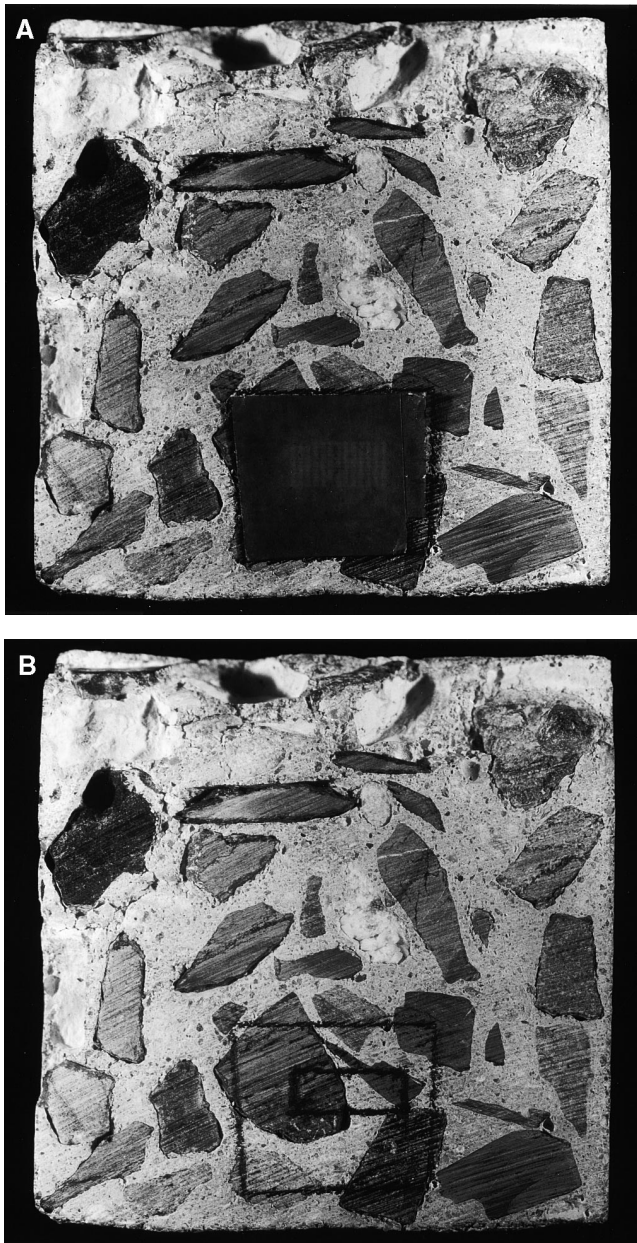


Fig. 2. Ordinary photographic display of the rectangular concrete block showing the largest 77×78 mm face uppermost: (a) with the X-ray beam sensitive paper still intact on surface; the actual beam traverse area is just about visible as 13 parallel stripes within the lighter central region; (b) with the X-ray beam sensitive paper removed but the outlines of the paper (outer rectangle) and the traverse area (inner rectangle) marked in pencil.

volume of the specimen. Consequently, it was decided to apply TEDDI to this problem.

The 1×2 -in. cores drilled from the prisms are the ideal size and shape for TEDDI examination. Cores were available for the concrete batches for the two lowest levels of potassium content. For the highest level of potassium, it was necessary to cut a 1-in. slice off the end of one of the prisms. The first results of the TEDDI analysis of this concrete piece are reported here.

3. TEDDI configuration

Initial tests confirmed that high quality transmission EDD patterns could be collected within minutes along any principal direction including the longest axis, 77 mm, which is the greatest thickness penetrated by this technique to date. A rectangular 13×6 -mm area was selected on one of the external faces (Fig. 2a,b), on account that it contains mortar and parts of two aggregate particles of differing appearance. The concrete piece was set up on the TEDDI system (station 16.4 of the 6-T wiggler beamline of the SRS synchrotron at Daresbury, UK) in such a configuration to tomograph a rectangular volume starting from this surface area and extending inside the block (this volume is indicated schematically in Fig. 1). The energy-dispersive detectors were set at 2θ -angles of 2.399° , 5.138° , and 7.911° and the diffracting lozenges were 0.5 mm in diameter by 13.1, 6.67 and 4.3 mm in length, respectively. A 2D tomographic scan was set in motion in which the external limit of the longest (13.1 mm) diffraction lozenge traversed the 13×6 -mm area in 13×13 steps: the position of the scanned area is indicated using X-ray sensitive paper placed on the concrete surface (Fig. 2a). The collection time at each point was 300 s, this amounting to an overall scan time of just over 14 h.

4. Results

Although the aim of this study was to yield point by point tomographic information, we also note the sheer size

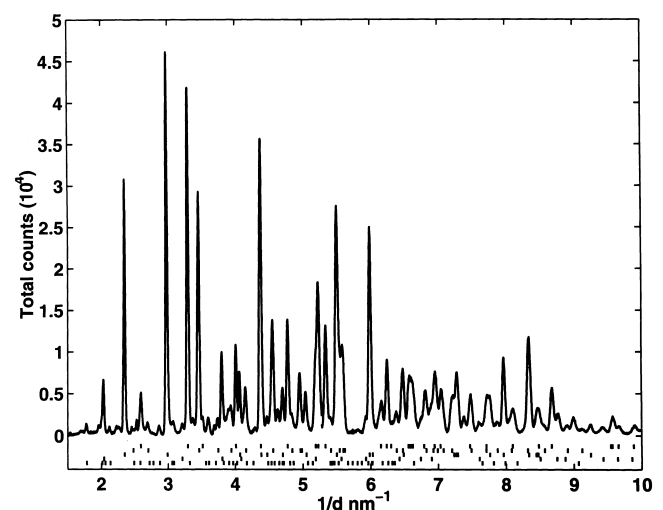


Fig. 3. A unique pattern form of EDD data obtained by summing all 507 patterns (after background subtraction) obtained over the complete tomographic traverse and merging the $1/d$ -range contributions from each of the three detectors. The result is a high quality pattern (10^7 – 10^8 photons) covering nearly an order of magnitude range in reciprocal space (1.5 – 10 nm^{-1} ; equivalent to ~ 1 – 7 Å d -spacings) and representing a bulk $13 \times 13 \times 6$ mm³ volume of concrete. The five rows of tick marks represent the expected peak positions for the five dominant crystalline phases, from top to bottom: calcite, dolomite, quartz, portlandite, and ettringite.

of a 14-h scan, encompassing some 10^8 scattered/diffracted photons, yielding a 2.1-Mb data set, and being representative of a sizable specimen volume ($\sim 1000 \text{ mm}^3$, or 1 cm^3); as such, it amounts to a truly bulk-averaged result with high counting statistics. One can distill all this diffraction information from the three detectors into one single plot

provided the patterns are expressed in units of reciprocal space ($1/d$) rather than photon energy (this is shown in Fig. 3), the final pattern covering nearly an order of magnitude range in reciprocal space, and representing a truly bulk volume ($\sim 1000 \text{ mm}^3$) of concrete. The five rows of marks show the expected peak positions for the five dominant crystalline phases, from top to bottom: calcite, dolomite, quartz, portlandite, and ettringite, which together account for 98% of the diffracted intensity.

The individual TEDDI maps are shown in Fig. 4 for the four main phases. The two aggregate regions, which can also be seen by their surface projection in Fig. 2b, are readily apparent. Both aggregates, particularly the larger aggregate, appear to be a physical mixture from both the dolomite and calcite source materials. With regard to cement content, one must note that, since TEDDI is a diffraction-based technique responding primarily to *microcrystalline* material, the semi-amorphous C–S–H gel developed from Portland cement will not be readily apparent; however, the accompanying hydrate, calcium hydroxide (portlandite) being microcrystalline is readily identified in the intervening cementitious region between the aggregates (Fig. 4c). The composition gradients evident at the aggregate/cement boundaries are subject to averaging over the third *depth* dimension perpendicular to the block surface: that is, the aggregate boundaries in the 2D plane parallel to the block surface will inevitably vary throughout the constant depth of this tomographic scan. As already stated, the presence of ettringite in this sample was anticipated and the diffraction peaks for ettringite are indeed significant and reliable (Fig. 3). The ettringite map (Fig. 4d) confirms the expected location of ettringite in between the aggregates, closely following the portlandite thus suggesting a fairly intimate mixture of the two. Small traces of thaumasite were possibly present but this was very difficult to ascertain from diffraction analysis due to overlap of the diagnostic peak with those of the abundant ettringite phase. Finally, it should be pointed out that the presence of dolomite in the coarse aggregate was unexpected. This type of aggregate is usually represented as pure limestone and therefore not expansive. However, TEDDI analysis has shown that it is present in this particular specimen and raises the question of whether

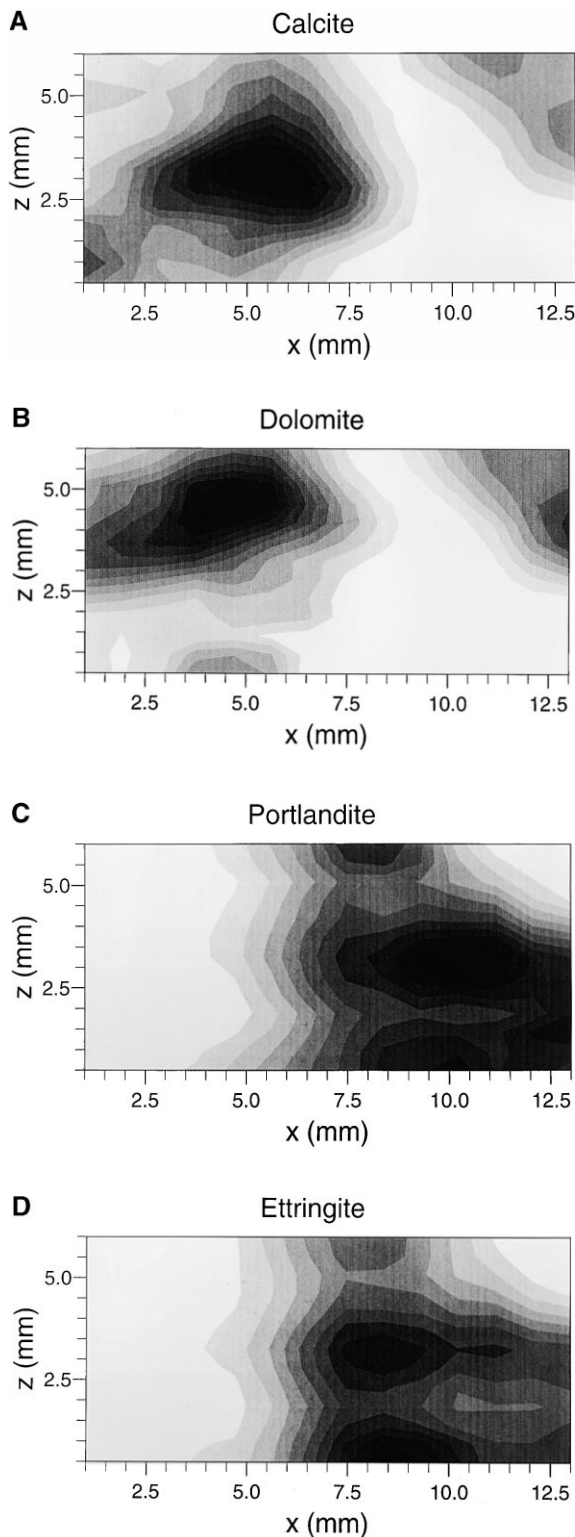


Fig. 4. A series of 2D-TEDDI-maps of a 13×6 -mm region, up to 13 mm in depth, under the concrete block surface (dark = high to white = low concentration): (a) the calcite map is obtained from the 104 diffraction peak at 3.04 \AA (45.50 keV) with the $2\theta = 5.138^\circ$ detector, indicating a large aggregate (bottom half) and the edge of a second aggregate (top left); (b) the dolomite map is obtained from the 104 diffraction peak at 2.90 \AA (47.69 keV) with the $2\theta = 5.138^\circ$ detector, producing very similar aggregate shapes to the calcite map; (c) the portlandite map is obtained from the 020 diffraction peak at 4.9 \AA (60.41 keV) with the $2\theta = 2.399^\circ$ detector, showing Ca(OH)_2 in the intervening cementitious region between the two calcite/dolomite aggregates; (d) the ettringite map is obtained from the 110 diffraction peak at 5.60 \AA (52.86 keV) with the $2\theta = 2.399^\circ$ detector, producing a very similar map to the portlandite, suggesting an intimate mixture of the two phases.

some of the expansion was produced by the dolomite through the alkali–carbonate reaction.

5. Conclusions and future studies

We have demonstrated that TEDDI is potentially a powerful technique for identifying the main microcrystalline constituents of concrete within a large sampling volume and for grading the concentration of these constituents on a sub-millimeter scale. Since the technique is non-destructive, at least for samples with thicknesses up to 50–80 mm, there is the future prospect of performing repeated TEDDI analyses on the same bulk specimen throughout its long-term hydration history (i.e., over years). In this way, we could envisage monitoring the hydration progression around precisely the same intergranular regions, from the earliest stages when the calcium silicate/alumino-ferrite phases are predominant to various hydration regimes where portlandite, ettringite, and monosulfate phases might be anticipated. Such samples could be stored, and even analyzed, under a variety of environmental conditions (temperature, humidity, surrounding solution, stress/load) so as to seek more definitive answers to long-standing problems such as delayed ettringite/thaumasite formation. The intention is also to push, in parallel, the technique at the microscopic end (1–100 μm scale) and find corresponding micro-applications for non-destructive TEDDI analysis in the field of cements.

Acknowledgments

We wish to thank the Research Councils (EPSRC, CLRC) for research grants and the use of synchrotron facilities, particularly Prof. D. Norman (Daresbury Laboratory) for granting discretionary beamtime, and the USA Federal Highway Administration for their help.

References

- [1] C. Hall, P. Barnes, J.K. Cockcroft, S.D.M. Jacques, A.C. Jupe, X. Turrillas, M. Hanfland, D. Hausermann, Rapid whole-rock mineral analysis and composition mapping by synchrotron X-ray diffraction, *Anal Commun* 33 (1996) 245–248.
- [2] H. He, P. Barnes, J. Munn, X. Turrillas, J. Klinowski, Autoclave synthesis and thermal transformations of the aluminophosphate molecular sieve VPI-5: An in-situ X-ray diffraction study, *J Chem Phys Lett* 196 (1992) 267–273.
- [3] S.M. Clark, A. Nield, T. Rathbone, J. Flaherty, C.C. Tang, J.S.O. Evans, R.J. Francis, D. O'Hare, Development of large volume reaction cells for kinetic studies using energy-dispersive powder diffraction, *Nucl Instrum Methods Phys Res, Sect B* 97 (1995) 98–101.
- [4] X. Turrillas, P. Barnes, D. Gascoigne, J.Z. Turner, S.L. Jones, C.J. Pygall, C.F. Pygall, A.J. Dent, Synchrotron-related studies on the dynamic and structural aspects of zirconia synthesis for ceramic and catalytic applications, *Radiat Phys Chem* 45 (1995) 491–508.
- [5] P. Barnes, X. Turrillas, A.C. Jupe, S.L. Colston, D. O'Connor, R.J. Livesey, P. Livesey, C. Hall, D. Bates, R. Dennis, Applied crystallography solutions to problems in industrial solid state chemistry: case examples with ceramics, cements and zeolites, *J Chem Soc, Faraday Trans* 92 (1996) 2187–2196.
- [6] S.L. Colston, S.D.M. Jacques, P. Barnes, A.C. Jupe, C. Hall, In-situ hydration studies using multi-angle energy-dispersive diffraction, *J Synchrotron Radiat* 5 (1998) 112–117.
- [7] L. Bailey, E. Boek, S. Jacques, T. Boassen, O. Selle, J.-F. Argillier, D. Longeron, Particulate invasion from drilling fluids, *Soc Pet Eng Paper No. 54762*, 1999, pp. 471–480.
- [8] D. Hausermann, P. Barnes, Energy-dispersive diffraction with synchrotron radiation: Optimisation of the technique for dynamic studies of transformations, *Phase Transitions* 39 (1992) 99–115.
- [9] R.A. Livingston, M.H. Manghnani, B.A. Clark, E.-S. Ramadan, Microstructural characterization of ettringite-associated damage in concrete, *Abstr Am Ceram 1999 Annu Meet* (1999) 350.
- [10] E. Grabowski, E. Czamecki, J.E. Gillott, C.R. Duggan, J.F. Scott, Rapid test of concrete expansivity due to internal sulfate attack, *ACI Mater J* 89 (1992) 469–480.
- [11] A.O.A. Ramadan, Development of a modified expansion test method for evaluating the potential for concrete DEF, PhD Thesis, Civil Engineering Department, University of Maryland, 1999, unpublished.